Ashish Bhave*, Stefan J. Rupitsch, Knut Moeller

Simplified inverse model for basic lumen shape identification

https://doi.org/10.1515/cdbme-2025-0182

Abstract: Narrowing and stiffening of arteries are a major cause for cardiovascular diseases such as heart attacks and hypoxia. A current inflatable balloon sensor system integrated on a guide catheter system is being developed to diagnose the degree of narrowing in vessels and its shape and determine localized tissue stiffness. The local 'tactile' strains on the balloon segments are intended to be converted into predictive assessment and decision aids for the surgeon. This contribution in the first step forward simulates in 2D an ideal balloon inflation within different rigid shapes of equal perimeter and captures the local stretch information from the balloon segments and the enclosed area of the balloon in the conformed state. This information serves as an input of an inverse model to create to estimate the tissue shape. The inverse model utilizes the difference of the individual segment stretches and the mean of segment stretches to compute the external angle formed by the segments. The reconstruction of the basic simulated lumen profiles is obtained with fairly accurate metrics though some discrepancies about the reconstructed area and accuracy of actual shape arise in few simulations. The study provides some information on the measurement sensitivity and the reconstruction and suggests some other refinement and techniques may be useful for reliable and accurate reconstruction.

Keywords: Inverse modelling, Identification, Tissue Biomechanics, Artery, PDMS sensor

1 Introduction

Treatment of narrowed pathological arteries has been one of the most common procedures performed all over the world.

*Ashish Bhave: Institute of Technical Medicine, Furtwangen University, Jakob Kienzle Str. 17, 78054, Villingen-Schwenningen, Germany. e-mail: bha@hs-furtwangen.de

Stefan J. Rupitsch: IMTEK, Faculty of Engineering Georges-Köhler-Allee 102, Freiburg, 79110 Germany.

Knut Moeller: Institute of Technical Medicine, Jakob Kienzle Str 17, 78054, Villingen-Schwenningen, Germany.

been performed since few decades. Cardiological interventions constitute major healthcare expenses. Current state of the art methods like angiography provide some information about location and extent of blockage. Methods like optical coherence tomography can show constitution of local tissue upto certain depth; IVUS can provide some stiffness information; MRI could provide 2D and 3D reconstruction but susceptible to motion artefacts and lower resolution.

Many procedures like bypass surgery, stenting, dilatation have

To assess the actual vessel lumen shape and the local tissue stiffness, development on a diagnostic in-vivo sensoractuator is currently under progress [1]. This sensor could provide tactile assessment that can be used to generate into decision aids for the doctor in real time.

Previous work has demonstrated that there is a correlation of local stretches on the balloon surface to the shape and curvature of the idealized lumen shapes [2, 3]. Techniques also show the overall tissue stiffness of vessels in-vivo could be estimated using model based identification techniques [4].

For conversion of sensor information into relevant shape information, a reliable and correct inverse identification procedure needs to be established. This contribution focusses on a simple formulation to convert the local strain changes captured on an ideal inflatable balloon systems in 2D and the area by the balloon for inverse modelling.

2 Methods

The aim of the paper was to use stretch data from the forward simulation of the idealized balloon sensor expansion within different lumen shapes and whether the devised inverse model can correctly identify those shapes uniquely from sensor data (and to what extent).

Geometry and Boundary conditions

COMSOL v6.3 was used for the forward modelling using Finite Element simulations. The perimeter of lumen(shapes) was ~19.45mm referring to an average iliac artery lumen diameter found in humans [5]. Basic ideal shapes of a circle, rhombus, square, rectangle, ellipses and 2 models with different degrees occlusion (indent models) were constructed and imparted stiffness >> balloon. The geometrical properties of the figures are provided in Table 1.

The balloon of diameter 4mm and with thickness $10\mu m$ was initialized with PDMS material properties [6, 7]. The outer boundary was equally divided into 128 elements (for higher information resolution) in circumferential direction as shown in Figure 1. The balloon is placed within the generated shapes. Pressure was applied on the inner boundary of this thin balloon and allowed to inflate upto 15kPa to conform sufficiently with the ideal inner boundary of the basic shapes. Relevant boundary conditions like spring, symmetry were applied for stable convergence and reducing degrees of freedom. Any time dependent effects were excluded in these relatively ideal simulations [7].

Furthermore, in actual experiments, the volume of liquid filling the balloon can be controlled and measured. In the simulations, volume could be converted into cross-section area enclosed by balloon and length (with the assumption that the balloon is longitudinally symmetrical) and was considered as an available measurement for use.

Table 1: The basic shapes and its features. All equate to approximately 19.45 mm perimeter.

Shape	Features				
Rhombus	Internal angles 120° and 60°, Side 4.86mm				
Rectangle	Longer Side 5.75mm shorter side 4mm				
Ellipse1	Major axis= 3.5mm, Minor axis= 2.66mm				
Ellipse2	Major axis= 4mm, Minor axis= 2.04mm				
Square	Side 4.86mm				
Indent1	Formula of indent based on Eq.17 and				
	Eq.18 in [8], indent depth 0.5 mm, healthy				
	part diameter 6.19 mm [5]				
Indent2	Formula of indent based on Eq.17 and				
	Eq.18 in [8], indent depth 2 mm, healthy				
	part diameter 6.19 mm [5]				

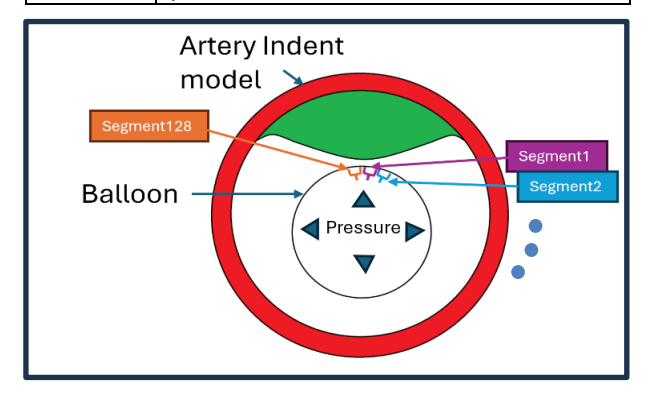


Figure 1: Balloon-in-vivo 2D interaction simulation. Stretch/strain data is collected through segments 1:128 which are initialitzed on the outer boundary of the balloon.

At the conformed shape, stretch data was extracted from these 128 balloon segments (segment 1 on balloon starting at the top and the following ones in clockwise direction as seen in Figure 1). The area enclosed by the balloon was also extracted.

Inverse modelling: We implemented a simple methodology for inverse identification and used MATLAB v2024 for data processing. An arbitrary starting point of the figure was considered where x,y coordinate were (0,0). Segments were to be plotted consecutively and were continuous (segments 1:128). The segment orientation is based on exterior angle formed by the selected segment with its previous segment. Di in Eq. 1 is formulated to be the exterior angle (Delta Angle deviation) that a segment forms to the adjacent segment (measuring anticlockwise). In our case i=1:1:128, and we generated 129 vertices. SegmentStretch constitutes the measured stretch of the balloon segment at 15kPa. Each reconstructed segment is enforced to be straight line of the given measured stretch value. 'Scale' is a scaling multiplier to the difference to be identified.

$$\begin{split} D_i &= -(\frac{360^\circ}{128} + \frac{\text{SegmentStretch}_{\text{i}} - \text{mean}(\text{segmentStretch}[1:128])}{\text{mean}(\text{segmentStretch}[1:128])} * \\ & scale) \end{split}$$

The 'error_{func}' in Eq. 2 was the error function to be minimized. The x and y coordinates of point 129 were aimed to be enforced to superimpose on x and y coordinates of point 1 and therefore ideally there could be only 128 points. This enforced the open loop to be a closed loop. The other part of the error function to be minimized is the reconstructed area of the polygon formed to the measured 'target_{area}'. Both parts were given an equal weightage.

$$error_{func} = abs \left(sqrt \left(x_{129} - x_1 \right)^2 + \left(y_{129} - y_1 \right)^2 \right) \\ + abs \left(reconstructed_{area} - target_{area} \right)$$
 (2)

Constraints were applied that the exterior angle may not exceed +180° or -180° for narrowing the search domain for the factor. Further a multistart algorithm with 1000 randomized start points was initialized for an attempt to converge to the global minimum. The value of 'scale' was identified for each of the balloon-lumen simulation given the above constraints.

3 Results and Discussion

About the pre-analysis: The shapes of lower complexity were used to observe the balloon expansion within a stiffer exterior to generate forward data for inverse model

reconstruction. The first 5 shapes were always internally concave structures (always bending inward w.r.t adjacent elements while the 'indent' models were convex-concave structures.

About the Simulation; The balloon was able to sufficiently inflate at pressure of 15kPa (A safe in-vivo pressure level for arteries in case of rupture of balloon) and conform >95% to the lumen shapes of the rigid objects. The balloon had limitations to squeeze into the sharp corners of rhombus, square and rectangle. It may be possible that with application of higher pressures the balloon may conform much more but this was not an essential aim of the study.

Table 2: The reconstructed values of area to the reconstructed area. The ideal distance difference between point 129 and point 1 should be 0*mm* (target difference).

Shape	Target_area	Reconstru	Difference	Factor 'scale'
	area) in	in mm²	pt. 1 in mm	[-]
	mm ²		pu I m mm	.,
Rhombus	20.29	20.49	0.046	3395
Rectangle	23.11	23.11	0.1	3308
Ellipse1	29.23	29.21	0.0006	3843
Ellipse2	25.62	25.54	0.03	3843
Square	23.52	23.55	0.05	3477
Indent	25.1	26.05	0.04	1767
Indent2	25.17	23.49	0.11	4341

For each simulation, the values of the distance, difference between actual area and reconstructed area and sharp are found in Table 2. Reconstruction was obtained for all the selected shapes and the comparison with the actual shape is found in figure 2.

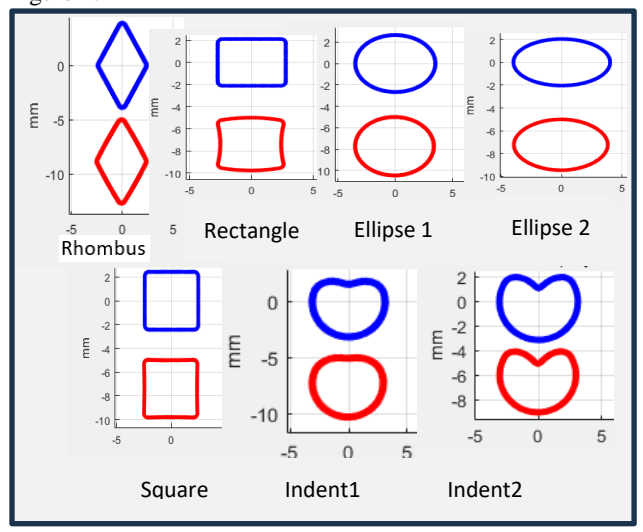


Figure 2: The in-silico shape of the balloon at 15kPa for different shapes in blue. The inverse reconstruction in red. Discrepancies in Rectangle and Indent reconstructions

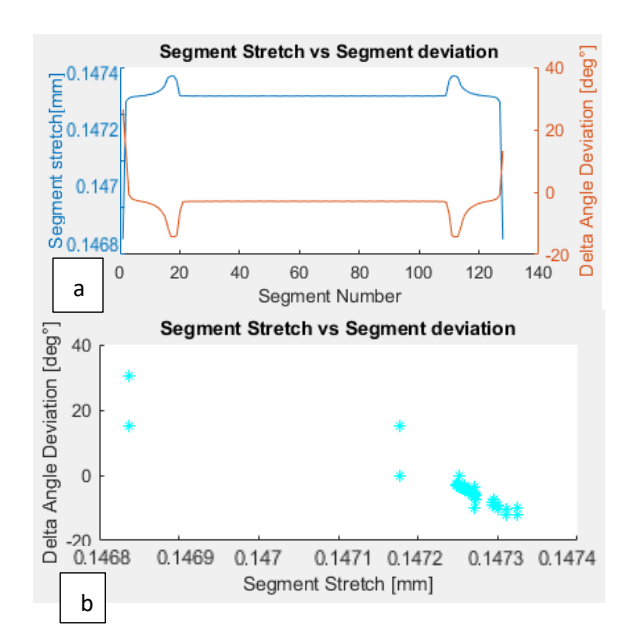


Figure 3: The first sub figure 2.a portrays Segment stretch and Delta angle deviation of segments for the corresponding segment number on the balloon when in indent 2 model. Fig 2.b displays segment stretch vs the Delta angle deviation and shows inverse relation but also different delta angle deviation for the identical stretch value.

About the selection of formula: While performing 2D simulations of balloon inflation without any surrounding tissue, it can be easily inferred that the stretch of the initially equal segments will be equal even post inflation and that the balloon still keeps the form of a circle. In our simulated case, the initial length of each element was equal and represented a delta angle deviation of $-360^{\circ}/128$ (segments bending inwards w.r.t the adjacent element). This value was added as a constant for each individual computation of D_i . The second part of equation 1 represents the deviation fraction of the element length to the mean stretch of elements (here at 15kPa). By simple computation it is be observed that the sum of the external angles will always be -360° (360° when clockwise frame of reference) and will conform to the general rule that sum of all external angles of a polygon is equal to 360°

About the Reconstruction: The error function assigns equal weightage to the area and to the closing of the segments into a loop. In the reconstructed balloon shape, an area error difference 1% percent to the actual balloon area is observed with the exceptions of the indent models where it is larger. Inspite of the good area and distance metric, we see differences in final reconstruction in the indent models and the rectangle. There are slight inaccuracies in reconstructed area in indent models, but the closing of loop is largely accurate in all models. Perhaps tuning the weightage in the error functions can result in better outcome.

About the correlation of stretch values to the segments :

We observe the correlation of the stretch of the balloon elements to the curvature of the lumen/boundary of the object as also seen in Bhave et.al [3]. In Figure 2.a we observe example of the segment stretch to it's the external angle in case of indent 2 model simulation. With fairly good resolution of simulation (due to large number of sensing balloon elements), differences can be relatively observed and comprehended.

About the shape identification accuracy: As observed in Figure 2.b, different external angles exist for the same amount of stretch. Therefore, the current approach is an approximation and could be refined later by perhaps by averaging D_i over elements on both sides of selected element. Sharp bends may require higher resolution, but as such may be difficult to find intra-luminal. It is possible we may influence the accuracy of reconstruction by tweaking the reconstruction algorithm. With even higher number of sensing elements divisions on balloon, it may be possible to further accurately resolve the shape but may be limited by the currently available and practical manufacturing capabilities.

About sharp factor: The 'scale' factor scales the deviation of the stretch of the element w.r.t to its mean value and can be seen that it is not unique for the all simulations. It is also evident from the data that 'scale' may not be directly correlated with the area enclosed by the balloon. Total Lumen Perimeter (for e.g. in highly narrowed vessels) and the sharpness of the curvature may have a bearing on the identified results and needs further investigation. Multiple situations exist where adjacent elements may have equal values in a very small tolerance range; one, that the local sensing elements may have conformed to a generally flat surface; two, that the curvature conforms to a concavity of a perfect circle or three, that the balloon might not have conformed to a certain region but just bulging. Given all these aspects, the reconstruction of the shape can be challenging.

4 Conclusion

The basic formulation attempted in this paper is a first step of identifying shape of the lumen of a calcified/pathological vessel and shows a promising outcome. By using the area enclosed by the balloon in 2D, we approximated the volume to be uniformly distributed over length. In 3D simulations with asymmetric lumen and different local tissue properties, the above approximation might strongly influence the inverse modelling.

Further research can show the optimal number of elements required for reconstruction. Refinement in the identification procedure may be possible, and its improvement and robustness can be important intermediate step to create live decision aids to a vascular surgeon. More realistic boundary conditions in FEM and later looking at influence of signal noise on reconstruction will be part of the upcoming work.

Author Statement

The support of Furtwangen University student Gayathri Avulupati is appreciated in data sorting for simulation. Research funding: This research was partly supported by the German Federal Ministry of Research and Education (BMBF) under grant no. 13FH066KX2 (DiaKatPlus/FH-Kooperativ) Conflict of interest: Authors state no conflict of interest. Informed consent: Informed consent has been obtained from all individuals included in this study. Ethical approval: No ethical approval required.

References

- Sittkus B, Zhu R, Mescheder U. Flexible piezoresistive PDMS metal-thin-film sensor-concept for stiffness evaluation of soft tissues. In: 2019 IEEE International Conference 7/2019. p. 1–3. doi:10.1109/FLEPS.2019.8792278.
- [2] Bhave A, Sittkus B, Rupitsch SJ, Mescheder U, Moeller K. Finite Element Analysis of a High Compliant Balloon with Strain Sensing Segments for the Identification of Biomechanical Properties within Tubular Vessels. IFAC-PapersOnLine. 2023;56:8242–7. doi:10.1016/j.ifacol.2023.10.1008.
- [3] Bhave A, Rupitsch SJ, Moeller K. Analysis of stretch distribution of high compliant elastomers within folded lumen vessels. Current Directions in Biomedical Engineering. 2023;9:686–9. doi:10.1515/cdbme-2023-1172.
- [4] Bhave A, Sittkus B, Rupitsch SJ, Knut Moeller. Evaluation of high compliant elastomer balloons for the identification of artery biomechanics 2023. doi:10.18416/AUTOMED.2023.
- [5] Ahn H-Y, Lee H-J, Lee H-J, Yang J-H, Yi J-S, Lee I-W. Assessment of the optimal site of femoral artery puncture and angiographic anatomical study of the common femoral artery. J Korean Neurosurg Soc. 2014;56:91–7. doi:10.3340/jkns.2014.56.2.91.
- [6] Bhave A, Rupitsch SJ, Moller K. Simulation study of inflation of a high compliant balloon inside idealized non-linear tissue geometry. Current Directions in Biomedical Engineering. 2022;8:672–5. doi:10.1515/cdbme-2022-1171.
- [7] A Bernardi L, Hopf R, Ferrari A, Ehret AE, Mazza E. On the large strain deformation behavior of silicone-based elastomers for biomedical applications. Polymer Testing. 2017;58:189–98. doi:10.1016/j.polymertesting.2016.12.029
- [8] Bhave A, Sittkus B, Urban G, Mescheder U, Möller K. Finite element analysis of the interaction between high-compliant balloon catheters and non-cylindrical vessel structures: towards tactile sensing balloon catheters. Biomech Model Mechanobiol. 2023;22:2033–61. doi:10.1007/s10237-023-01749-8.